AIP Advances

The vacuum UV photoabsorption spectroscopy of the cis-1,2-dichloroethylene (1,2-ClHC=CHCl) in the 5-20 eV range. An experimental and theoretical investigation

Cite as: AIP Advances **9**, 015305 (2019); https://doi.org/10.1063/1.5066368
Submitted: 15 October 2018 . Accepted: 21 December 2018 . Published Online: 11 January 2019

R. Locht, D. Dehareng, and B. Leyh

The vacuum UV photoabsorption spectroscopy of the cis-1,2-dichloroethylene (1,2-ClHC=CHCl) in the 5-20 eV range. An experimental and theoretical investigation

Cite as: AIP Advances 9, 015305 (2019); doi: 10.1063/1.5066368
Submitted: 15 October 2018 • Accepted: 21 December 2018 •
Published Online: 11 January 2019

R. Locht,[1,a)] D. Dehareng,[2] and B. Leyh[1]

AFFILIATIONS

[1] UR MolSys, Molecular Dynamics Laboratory, Department of Chemistry, Building B6c, University of Liège, Sart-Tilman, B-4000 Liège 1, Belgium

[2] Center for Protein Engineering, Department of Life Sciences, Building 6a, University of Liège, Sart-Tilman, B-4000 Liège 1, Belgium

[a)] **Corresponding author:** Tel. +32 4 366 3520: Fax: +32 4 366 3413; **E-mail address:** robert.locht@ulg.ac.be (R. Locht)

ABSTRACT

The photoabsorption spectrum of cis-1,2-$C_2H_2Cl_2$ has been examined in detail in the vacuum UV range between 5 eV and 20 eV photon energy by using synchrotron radiation. Quantum chemical calculations are proposed and applied to the electronic transitions and to the vibrational structures belonging to these transitions. The broad band observed at 6.568 eV includes the $\tilde{X}^1A_1 \rightarrow 1^1B_1$, 3^1B_2 and 2^1B_1 transitions. The two latter excitations correspond to the valence $2b_1(\pi) \rightarrow \pi^*$ and to the Rydberg $2b_1(\pi) \rightarrow 3s$ transitions. The former excitation is described by a more complex $2b_1(\pi) \rightarrow n_{Cl} + \sigma^*_{CH}/Rp\sigma$ transition where valence and Rydberg characters are strongly mixed. For these transitions short vibrational progressions are observed, analyzed and tentatively assigned. The abundant structure observed between 7.0 eV and 10.0 eV has been analyzed in terms of vibronic transitions to one ns- ($\bar{\delta}$ = 0.960), two np- ($\bar{\delta}$ = 0.525 and 0.337), and two nd-type ($\bar{\delta}$ = 0.080 and 0.002) Rydberg series, all converging to the $\tilde{X}^2B_1$ ionic ground state. The vibrational structure analysis of the Rydberg states leads to the following average wave numbers: $\omega_2 \approx 1420$ cm^{-1} (C=C stretching), $\omega_3 \approx 1190$ cm^{-1} (symmetric C-H bending), $\omega_4 \approx 800$ cm^{-1} (symmetric C-Cl stretching) and $\omega_5 \approx 190$ cm^{-1} (symmetric C-Cl bending). These numbers are compared to previously reported values. Many other transitions are observed between 10 eV and 20 eV and are assigned to transitions to Rydberg states converging to the successive excited states of cis-1,2-$C_2H_2Cl_2^+$. For several of these Rydberg states, a vibrational structure is also observed and interpreted.

I. INTRODUCTION

The chlorinated derivatives of ethylene are important reactants in several industrial applications. They are also used to replace long-living ozone-depleting agents.[1] As a consequence, these compounds became widely spread but were found to be abundant atmospheric air pollutants.[2] Their toxicity and potential carcinogenicity have been investigated.[3] Several groups studied the release of the highly ozone-depleting Cl atom and HCl molecule by UV photons[4–6] or atmospheric OH attack[7,8] in the three isomers of dichloroethylene. Gas-phase ion chemistry of these compounds has also been reported.[9] These aspects were almost only investigated in the two 1,2-$C_2H_2Cl_2$ isomers. However,

the studies on the photoabsorption spectrum of both compounds remain scarce and mainly restricted to the 160-135 nm (or 7.75-9.18 eV) wavelength region.

The first vacuum UV photoabsorption spectrum (PAS) of the two 1,2-$C_2H_2Cl_2$ isomers has been reported by Mahncke and Noyes[10] in 1935. They recorded the spectra between the visible region and 75 nm (16.53 eV). They roughly divided them into three parts: (i) a broad continuum starting at 240 nm (5.17 eV) with a maximum at 190 nm (6.52 eV), (ii) a discrete absorption spectrum extending from 157 nm (7.90 eV) to 135 nm (9.18 eV) and (iii) a continuous absorption below 128 nm (9.69 eV) in the cis-isomer and a series of diffuse bands in the trans-isomer. A Rydberg series classification and a vibrational analysis were attempted. Ionization energies were obtained by Rydberg series extrapolation.

Walsh[11] recorded the vacuum UV PAS of all chloroethylenes, except the 1,1-$C_2H_2Cl_2$ species. Beside the broad continuum peaking at 185-195 nm (6.70-6.36 eV), vibrational progressions of different Rydberg series were observed and analyzed in all spectra.

Walsh and Warsop[12] reported a detailed analysis of the vacuum UV PAS of the cis-1,2-$C_2H_2Cl_2$. They mention the continuum peaking at 190 nm (6.52 eV) but their attention was focused on the analysis and discussion of the discrete spectrum measured between 167 and 143 nm (7.42-8.67 eV).

In a paper on the photochemical HCl-loss from chloroethylenes, Berry[4] measured the vacuum UV absorption spectrum of all chlorinated derivatives of ethylene in the 260-140 nm range (4.77-8.86 eV) and analyzed in more detail the broad band located between 240 and 180 nm (5.17-6.88 eV). The discrete part of the spectrum has not been analyzed.

Closely related to photoabsorption spectroscopy, the low electron energy-loss spectroscopy of all chloro-substituted ethylenes $C_2H_xCl_{4-x}$ has been reported by Koerting et al.[13] This work was essentially focused on the singlet-triplet valence transitions. Excitations to singlet valence and Rydberg states below 7.0 eV were also observed.

On the quantum chemical level, Arulmoziraja et al.[14] presented an extended high-level theoretical study on the electronic transitions in the cis- and trans-dichloroethylenes, and in tetrachloroethylene using the SAC-CI theory. The main purpose was to obtain the electronic spectra and to assign excitations to valence and Rydberg states of both singlet and triplet multiplicity. More recently, Khvostenko[15] reported DFT calculations at the B3LYP/6-311-G(d,p) level of the transitions to excited valence singlet and triplet states of chloroethylene molecules.

We recently reported on the vacuum UV PAS study of 1,1-$C_2H_2Cl_2$[16] observed and analyzed between 5 eV and 20 eV photon energy. In the frame of our work on this series of molecular systems, the aim of the present paper is to propose a detailed analysis of the vacuum UV photoabsorption spectrum of the cis-1,2-$C_2H_2Cl_2$ isomer (i) at medium resolution but for the first time in the 10-20 eV photon energy range and (ii) at higher resolution between 5.0 and 13.0 eV, with vibrational structure analysis. Quantum chemical calculations will be used to support the assignments. In a near future a similar work on the trans-1,2-$C_2H_2Cl_2$ isomer will be reported.[17]

II. EXPERIMENTAL

The experimental setup used in this work at the BESSY I and II synchrotron radiation facilities (Berlin, Germany) has been described previously.[18] Briefly, two monochromators have been used. For medium resolution spectra (resolving power of 1200 at hν = 10 eV), a modified 1.5 m-NIM 225 McPherson monochromator equipped with a 1200 lines/mm gold-coated laminar Zeiss grating was used. High resolution measurements (resolving power of about 15000 at 10 eV) have been reached with a 3m-NIM monochromator equipped with an Al/MgF_2 spherical grating of 600 lines/mm.

The synchrotron radiation intensity and the pressure inside the cell were monitored, ensuring reliable absorption data. The sample pressure was kept in the 30-40 μbar to prevent saturation. The cis-1,2-$C_2H_2Cl_2$ sample purchased from Aldrich (99% stated purity) was used without further purification.

As described and discussed in detail in previous works, a continuum subtraction procedure has been applied to better identify and characterize weak and/or diffuse structures superimposed on an intense continuum.[19,20] The resulting spectrum is denoted as Δ-plot. This data handling procedure has been validated by Marmet[21] and Carbonneau.[22]

The wavelength scales calibration is based on the Ar absorption spectrum between the $^2P_{3/2}$ and the $^2P_{1/2}$ ionic states, with an accuracy better than 2 meV. Between 6 eV and 20 eV photon energy, the photoabsorption spectrum has been recorded with energy increments of 15 meV, so that the energy

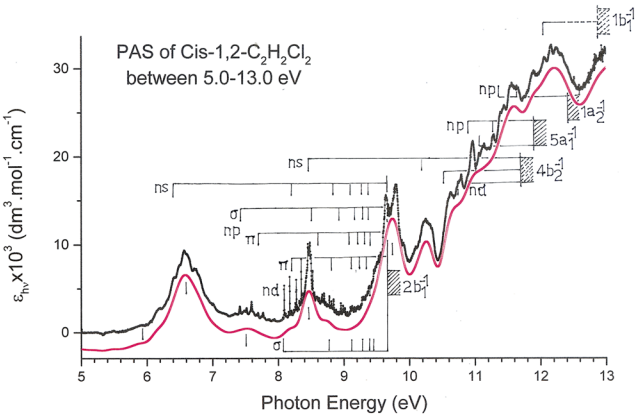

FIG. 1. Vacuum UV photoabsorption spectrum of cis-1,2-$C_2H_2Cl_2$ between 5 eV and 13 eV photon energy. The continuous red curve corresponds to the strongly smoothed PAS curve by fast Fourier transform. Vertical bars locate valence and Rydberg transitions and shaded areas show their convergence limit. Dotted areas correspond to vertical ionization energies.

positions have an uncertainty of about 8 meV. The 5-15 eV range has also been investigated with energy increments of 2 meV. Several parts of the spectrum, e.g., 7.0-10.0 eV and 11.6-12.2 eV, have also been recorded with 500 μeV energy steps. The energy positions are here known within ±2 meV. Reproducibility of energy positions has been checked with spectra recorded over several years.

III. EXPERIMENTAL RESULTS

Fig. 1 displays the vacuum UV PAS of cis-1,2-$C_2H_2Cl_2$ between 5 eV and 13 eV photon energy, with 2 meV energy increments.

The whole 5-20 eV range may be split in four distinct regions: (i) the 5.0-7.2 eV region consists of a number of weak broad bands superimposed on a continuum; (ii) the 7.2-9.6 eV range contains a large number of weak to very weak sharp features and bands superimposed on a relatively weak continuum with steeply increasing intensity starting at 9.2 eV; (iii) the region above 9.2 eV and up to 13 eV consists of a series of weak, fairly narrow structures superimposed on a strong continuum; (iv) the spectral range above 13 eV is displayed in Fig. 2a and consists of several successive broad bands up to 20 eV; the corresponding Δ-plot is displayed in Fig. 2b. The positions of the Rydberg transitions and the convergence limits[23] are identified.

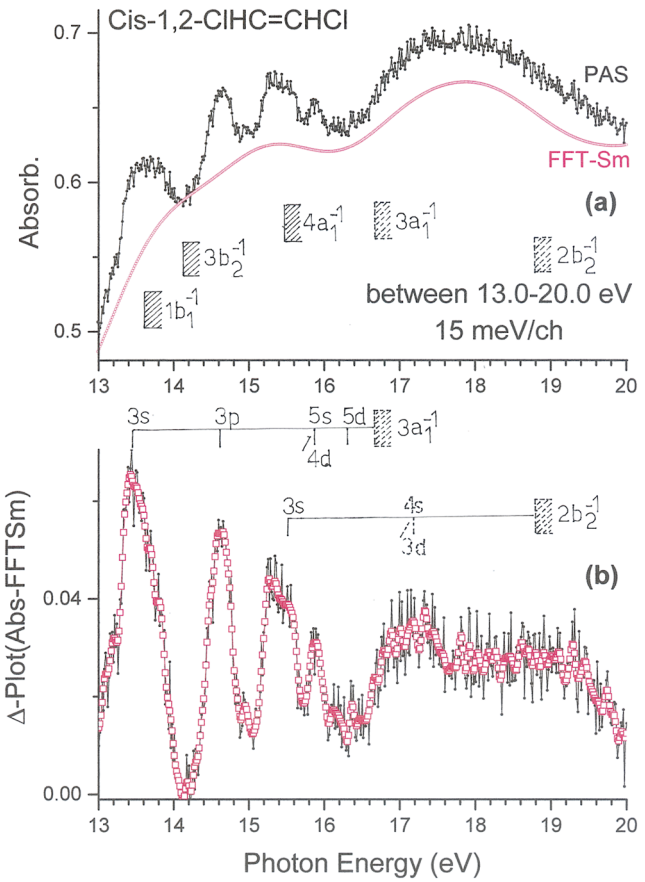

FIG. 2. Vacuum UV photoabsorption spectrum of cis-1,2-$C_2H_2Cl_2$ in the 13 - 20 eV range: (a) direct absorbance spectrum as recorded with the 1.5 m NIM monochromator, (b) Δ-plot. The red curve (FFTsm) corresponds to slightly smoothed data. Vertical bars indicate the band maxima and shaded areas correspond to the ionization energies of cis-1,2-$C_2H_2Cl_2$. Dotted areas correspond to vertical ionization energies.

Tables I and II list the energies of the vibrationless transitions to Rydberg states converging respectively to the ground

TABLE I. Rydberg series observed in the vacuum UV photoabsorption spectrum of cis-1,2-$C_2H_2Cl_2$ converging to the $\tilde{X}^2B_1$ (cis-1,2-$C_2H_2Cl_2^+$) ionic ground state at 9.666 eV. Energy positions (eV), wavenumbers (cm^{-1}), effective quantum numbers (n^*), average quantum defects ($\bar{\delta}$) and assignments as proposed in this work (1 eV= 8 065.545 cm^{-1}[24]). Comparison is made with the literature data of Refs. 10–12.

This Work			10	11	12
eV	cm^{-1}	n^*		cm^{-1}	
$2b_1 \rightarrow ns$ ($\bar{\delta}$=0.96±0.01)					
6.398	51603	2.040	-	-	-
8.192	66077	3.039	66020	65840	[65870]
8.836	71267	4.049	71220	71652	[70736]
9.130	73642	5.041	73652	73652	[73357]
9.295	74969	6.056	74954	74941	[74810]
9.390	75711	7.021			[75648]
$2b_1 \rightarrow np\sigma$ ($\bar{\delta}$=0.53±0.01)					
7.414	59798	2.458			59734
8.547	68936	3.487	69060		
8.985	72469	4.470	72408		
9.214	74316	5.486	74240		
9.340	75332	6.460			
9.424	76010	7.498			
$2b_1 \rightarrow np\pi$ ($\bar{\delta}$=0.34±0.02)					
7.740	62427	2.658	62605		
8.643	69710	3.647	69796		69847
9.045	72953	4.681	72957		
9.245	74566	5.685	74590		
9.357	75469	6.636	75437		
9.435	76048	7.674			
$2b_1 \rightarrow nd\sigma$ ($\bar{\delta}$=0.08±0.03)					
8.089	65242	2.918	65260	65182	
8.777	70791	3.912	70717	70725	70736
9.097	73396	4.903	73328	73331	
9.274	74816	5.907	74843	74749	
9.383	75655	6.897		75575	
9.449	76211	7.992			
9.495	76582	8.920			
$2b_1 \rightarrow nd\pi$ ($\bar{\delta}$=0.002±0.008)					
8.170	65895	3.015			[65870]
8.806	71025	3.978			[70736]
9.123	73582	5.006			[73357]
9.284	74880	5.999			[74810]
9.380	75655	6.996			[75648]

TABLE II. Rydberg series converging to the ionic excited states observed in the vacuum UV photoabsorption spectrum of cis-1,2-$C_2H_2Cl_2$. Energy position (eV), wavenumber (cm^{-1}), effective quantum numbers (n^*) and assignments proposed in this work. The IE's used as convergence limit[23] are IE_{vert} for $4b_2^{-1}$, $3a_1^{-1}$ and $2b_2^{-1}$ are 11.690 eV, 16.732 eV and 18.8 eV and IE_{ad} for $5a_1^{-1}$, $1a_2^{-1}$ and $1b_1^{-1}$ are 11.965 eV, 12.375 eV and 13.592 eV successively. Conversion factor: 1 eV = 8 065.545 cm^{-1}.[24]

eV	cm^{-1}	n^*	Assign.
	$4b_2\rightarrow$[a]		
8.446	67791	2.050	3s
10.252	82010	3.075	4s
10.584	84430	3.507	4p(π)
10.792	86527	3.892	4d
	$5a_1\rightarrow$		
10.880	87753	3.541	4p
11.120	89689	4.013	5s/4d
11.275	90939	4.441	5p(σ)
11.536	93044	5.631	6p(π)
	$1a_2\rightarrow$		
11.342	91479	3.629	4p(π)
11.750	94770	4.666	5p(π)
	$1b_1\rightarrow$		
12.054	97222	3.041	4s/3d
	$3a_1\rightarrow$[a]		
13.39	108000	2.02	3s
14.65	118160	2.56	3p
15.85	127840	3.93	4d/5s
16.15	130260	4.84	5d
	$2b_2\rightarrow$[a]		
15.55	125420	2.03	3s
17.30	139534	2.97	4s/3d

[a]The vertical ionization energy is used as convergence limit for these series.

and to excited ionic states. Previous data from the literature are also mentioned.[10–12]

IV. AB INITIO CALCULATIONS: METHODS AND RESULTS

A. Computational tools

Quantum chemical calculations were performed with the Gaussian 09 program package.[25] The aug-cc-pVDZ basis set containing polarization as well as diffuse functions[26] was used throughout. In specific cases, calculations with the basic cc-pVDZ set, which does not include diffuse functions, were also performed.

Geometry optimizations have been performed at the CCSD(FC),[27,28] DFT(M06-2X)[29] and TDDFT[30] levels.

The wavenumbers of the twelve vibrational normal modes were computed at the DFT(M06-2X) and TDDFT(M06-2X) levels.

B. Results of the calculations

The results of the geometry optimizations in the C_{2v}, C_2 and C_S symmetry point groups at different computational levels are presented in Table S1 (see supplementary material). These results are compared and discussed below.

The calculated vertical transition energies to several neutral excited states are listed in Table III with respect to the neutral ground state in the C_{2v} symmetry group. Only those neutral states excited with non-zero oscillator strength are mentioned.

The two lowest $^1B_1$ excited states calculated at the TDDFT level show a mixed character involving similar configurations but with different weights. For the 1^1B_1 at 5.98 eV, the main character is R'p'σ (where R stands for "Rydberg state") with an important [$n_{Cl}+\sigma^*_{CH}$] component whereas for the 2^1B_1 at 6.35 eV the R's' character is dominant with a smaller [R'p'σ+nCl+σ*CH] component. These states are therefore expected to be strongly coupled but this coupling is probably overestimated at the TDDFT level, leading to a very low energy for the first state. The first $^1B_2$ excited state, however, corresponds to a nearly pure π→π* configuration and has by far the largest oscillator strength.

The vibrational wavenumbers associated with the twelve normal modes represented in Fig. 3 have been calculated for the first four excited states of the neutral molecule at the

TABLE III. Vertical excitation energies (eV) leading to neutral excited states of cis-1,2-$C_2H_2Cl_2$ as obtained at the TDDFT level and description of the transitions involved. The corresponding calculated oscillator strengths are indicated in parentheses. The calculations were performed with the aug-cc-pVDZ basis set. The notation R stands for "Rydberg state".

Neutral State	E_{vert}(eV) TDDFT (CCSD)	Description (Oscillator strength)
1^1B_1	5.98	$\pi\rightarrow Rp\sigma/[n_{Cl}+\sigma^*_{CH}]$ (0.0011)
2^1B_1	6.35 (6.21)	$\pi\rightarrow Rs/[Rp\sigma+n_{Cl}+\sigma^*_{CH}]$ (0.0027)
3^1B_2	6.55 (5.09)	$\pi\rightarrow\pi^*$ (0.3077)
5^1B_1	7.32	$n_{Cl}+\sigma_{CH}\rightarrow\pi^*$ (0.0011)
8^1B_1	7.44	$\pi\rightarrow Rp\sigma$ (0.0211)
11^1A_1	7.90	$\pi\rightarrow Rp\pi$ (0.0379)
12^1B_2	8.24	$n_{Cl}+\sigma_{CH}\rightarrow Rs$ (0.0463)
13^1A_1	8.44	$n_{Cl}+\sigma_{CC}+\sigma_{CH}\rightarrow Rp\sigma$ and $n_{Cl}+\sigma_{CH}\rightarrow Rp_y$ (0.0102)
14^1A_1	8.58	$n_{pz,Cl}+\pi_{C\text{-}Cl}\rightarrow\pi^*$ (0.0211)
15^1B_1	8.64	$\pi\rightarrow Rd_{y2}$ and $\pi\rightarrow Rp\sigma$ (0.0148)
17^1B_1	8.81	$\pi\rightarrow Rp\sigma$ and $\pi\rightarrow Rd_{y2}$ (0.0127)
18^1B_2	8.97	$\pi\rightarrow Rd_{yz}$ (0.0373)
20^1B_2	9.15	$n_{Cl}+\sigma_{CH}\rightarrow Rs+Rp\sigma$ and $n_{Cl}+\sigma_{CC}+\sigma_{CH}\rightarrow\pi^*$ (0.0112)

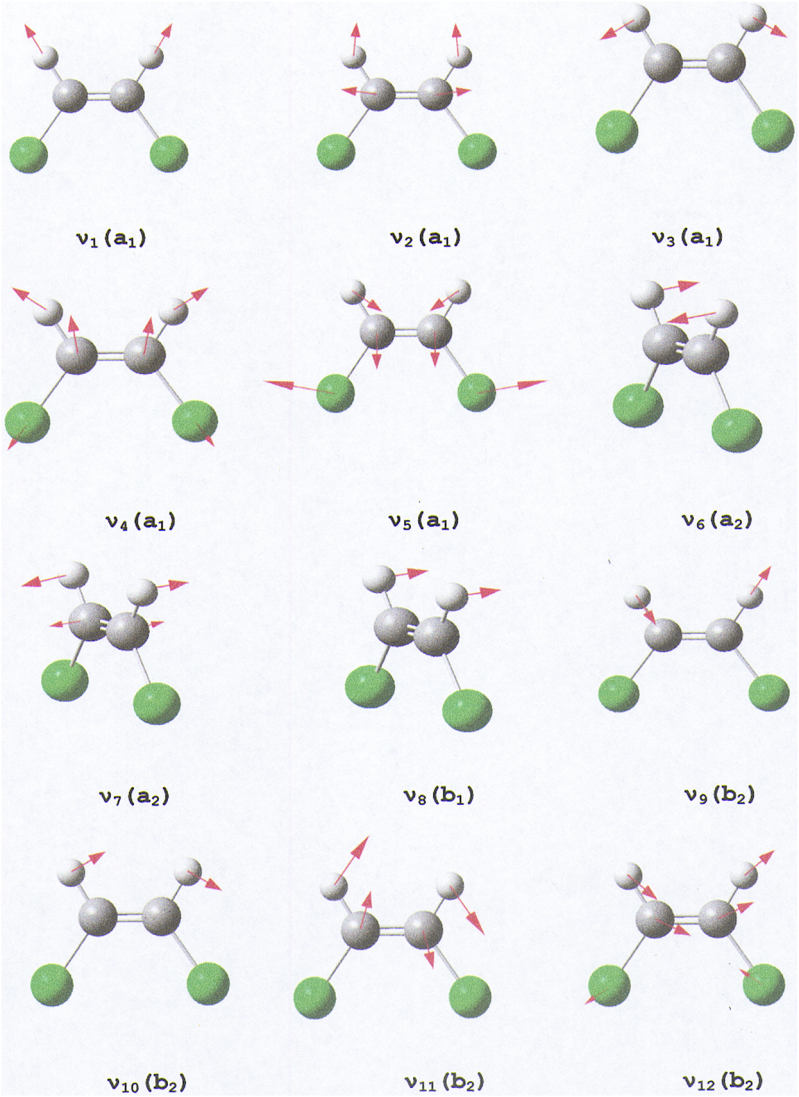

FIG. 3. Schematic representation of the twelve vibrational normal modes of the cis- 1,2-$C_2H_2Cl_2$ molecule in the C_{2v} symmetry point group (and their irreducible representations) for which the associated wavenumbers have been calculated.

TDDFT level in the C_{2v} symmetry group and are listed in Table IV. The presence of imaginary wave numbers indicates that these C_{2v} geometries do not correspond to equilibrium situations. Table V reports the vibrational wavenumbers of the neutral ground state in the C_{2v} group[31] and of the first $^1B_2$ excited state ($\pi \rightarrow \pi^*$) in the C_{2v},C_2 and C_S groups, computed at the DFT (M06-2X) level.

These optimizations of the 3^1B_2 excited state lead to an equilibrium geometry corresponding to a twisted situation of C_2 symmetry (all real wavenumbers, see Table V, column 5). In this geometry, the $\pi \rightarrow \pi^*$ state belongs to the ^1B representation. The C=C bond is moderately lengthened compared to the ground state but the bond angles are substantially modified (see Table S1). A saddle point is obtained in C_s (one imaginary wavenumber, see Table V, column 6) and a third order critical point in C_{2v} (stationary point with three imaginary wavenumbers, see Table IV, column 4 and Table V, column 4). Compared to the C_2 minimum, the stationary points in C_s and C_{2v} are destabilized by 1.13 eV and 1.24 eV, respectively. They are characterized by a very large C=C bond lengthening (nearly 0.2 Å) and large bond angle modifications.

Furthermore, at the optimized twisted C_2 geometry of the $3^1B_2/^1B$ state, the $\tilde{X}^1A$ state is higher in energy. Internal conversion from the ^1B state to the $\tilde{X}^1A$ state is expected to take place upon relaxation. Anticipating the publication of the calculation results on trans-1,2-$C_2H_2Cl_2$,[17] it can be emphasized that the 3^1B_2 optimized geometry is also that obtained from the optimization of the first excited state in the trans-isomer. It can therefore, be predicted that the isomerization is obviously photo-induced.

TABLE IV. Vibrational wavenumbers (cm^{-1}) calculated for the twelve normal modes (VNM) (see Fig. 3) of the first four excited states in the C_{2v} symmetry group at the TDDFT(M06-2X) level. For the neutral ground state comparison is made with experimental data.[31] Imaginary wavenumbers are bold printed.

State	1^1B_1	2^1B_1	3^1B_2	5^1B_1
VNM		a_1/a'		
ν_1	3279	3048	3293	3320
ν_2	1529	1427	1269	1470
ν_3	933	1205	1112	1083
ν_4	481	778	760	765
ν_5	147	159	189	270
		a_2/a''		
ν_6	840	901	**i 439**	**i 637**
ν_7	**i 297**	**i 420**	**i 964**	**i 766**
		b_1/a''		
ν_8	680	686	**i 738**	**i 728**
		b_2/a'		
ν_9	3251	3066	3281	3303
ν_{10}	1029	1359	1266	1164
ν_{11}	510	943	911	787
ν_{12}	**i 512**	553	484	485

TABLE V. Vibrational wavenumbers (cm^{-1}) calculated for the twelve normal modes (VNM) (see Fig. 3) of the neutral ground and first excited states in the C_{2v}, C_2 and C_S symmetry point groups at the DFT(M06-2X) level. For the neutral ground state comparison is made with experimental data.[31] Imaginary wavenumbers are bold printed.

State	C_{2v} $\tilde{X}^1A_1$		C_{2v} 3^1B_2	C_2 $3^1B_2/^1B$	C_s $3^1B_2/^1A''$	C_{2v} 1^1B_1
VNM				a_1/a'		
	Theor.	Exp.[31]				
ν_1	3242	3077	3297	3200	3189	3293
ν_2	1701	1587	1338	1356	1300	1488
ν_3	1190	1179	1136	1192	1122	944
ν_4	724	711	763	746	730	487
ν_5	171	173	181	120	183	158
				a_2/a''		
ν_6	908	876	**i 289**	522	571	800
ν_7	407	406	**i 517**	357	**i 431**	**i 506**
				b_1/a''		
ν_8	701	697	**i 448**	506	526	683
				b_2/a'		
ν_9	3219	3072	3285	3192	3171	3260
ν_{10}	1296	1303	1284	1168	1270	1016
ν_{11}	856	857	918	736	860	488
ν_{12}	571	571	495	352	432	**i 666**

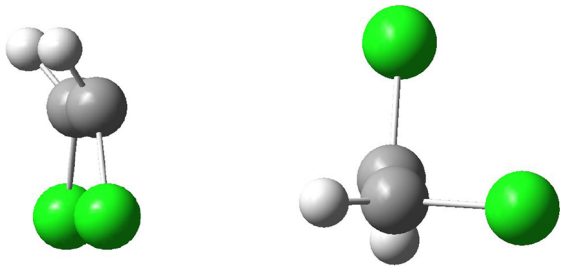

$1^1A''$ (TS) **1^1B state (min)**

Geometry optimizations in other symmetry point groups (C_s, C_2 and C_1) for the 1^1B_1 and 2^1B_1 states have been unsuccessful owing to the large variation of the electronic energies upon geometry change, leading to numerous crossings.

V. DISCUSSION OF THE EXPERIMENTAL DATA

In the C_{2v} point group, the molecular orbital configuration of cis-1,2-$C_2H_2Cl_2$ is given by

$$1s^2(Cl1)\ 1s^2(Cl2)\ 1s^2(C1)\ 1s^2(C2)\ 2s^2(Cl1)\ 2s^2(Cl2)\ 2p^6_{x,y,z}(Cl1) \times 2p^6_{x,y,z}(Cl2)\ 1a_1^2\ 1b_2^2\ 2a_1^2\ 2b_2^2\ 3a_1^2\ 4a_1^2\ 3b_2^2\ 1b_1^2\ 1a_2^2 \times 5a_1^2\ 4b_2^2\ 2b_1^2 : \tilde{X}^1A_1$$

where $1a_1$ is the deepest outer-valence shell orbital.

We recently measured the HeI-PES and threshold photoelectron spectra (TPES) of cis-1,2-$C_2H_2Cl_2$, which will be the subject of a forthcoming paper.[23] The lowest adiabatic ionization energy leading to cis-1,2-$C_2H_2Cl_2^+(\tilde{X}^2B_1)$ is equal to (9.666±0.006) eV. This value is in very good agreement with earlier[32–34] and with the most recent[35,36] determinations. The vertical value is measured at 9.843 eV.[23]

Eight bands were observed by HeI-PES at higher energies and were characterized by their adiabatic ionization energies at 11.426 eV, 11.965 eV, 12.375 eV, 13.592 eV, 14.083 eV, 15.531 eV and 16.638 eV and at about 18.40 eV.[23] The corresponding vertical values are 11.690 eV, 12.028 eV, 12.460 eV, 13.828 eV, 14.083 eV, 15.684 eV, 16.732 eV and about 18.8 eV successively.[23,32–34]

A. The valence transitions (Figs. 1, 4 and 5)

The characteristic low energy broad band observed in the vacuum UV PAS of the ethylene compounds displays a doublet maximum at 6.568 eV-6.620 eV in cis-1,2-$C_2H_2Cl_2$ (Fig. 4). Compared to our observations in the chlorinated derivatives investigated up to now,[16,37,38] this band has a similar intensity and extends between 5.3 eV and 7.3 eV. It results from the superposition of several contributions.

To enhance the weak structures superimposed on the continuum the subtraction method mentioned in Section II

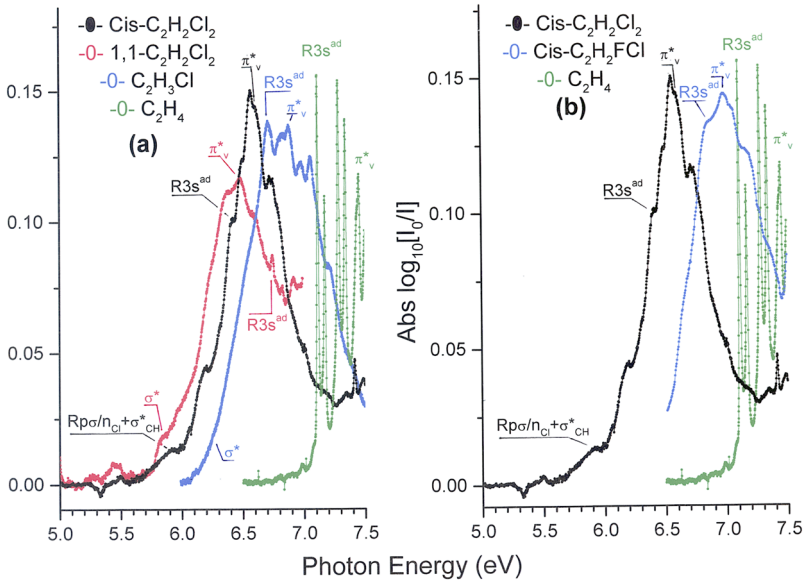

FIG. 4. Comparison of the 5.0-7.5 eV band in the vacuum UV photoabsorption spectra of C_2H_4 and the (a) three chlorinated ethylenes C_2H_3Cl, 1,1-$C_2H_2Cl_2$ and cis-1,2-$C_2H_2Cl_2$ and (b) the doubly substituted ethylenes cis-1,2-$C_2H_2Cl_2$ and cis-1,2-C_2H_2FCl. The valence (σ^* and π^*) and the Rydberg (R3s) transitions are indicated for each molecule.

has been applied. The red curve in Fig. 5a represents the continuum which is subtracted from the original signal. The result of this subtraction operation is displayed in Fig. 5b which clearly shows two different parts: (i) between 5.0 eV and 6.0 eV a very weak series of peaks with spacing suggesting a vibrational progression and (ii) between 6.0 eV and 7.0 eV a more intense series of alternating broad and narrow peaks.

The very weak signal between 5.0 eV and 6.0 eV may be interpreted as part of the transitions to a longer vibrational progression belonging to a singlet valence excited state. A $\pi\rightarrow\sigma^*$ state is a reasonable candidate. By quantum chemical calculations, Arulmozhiraja et al.[14] calculated the $\pi\rightarrow\sigma^*(1^1B_1)$ transition energy at 6.45 eV in cis-1,2-$C_2H_2Cl_2$ whereas Khvostenko[15] predicted this transition at 6.52 eV. The present calculations indicate a more complex situation where the final 1^1B_1 state has a strongly mixed Rydberg (R'p'σ) and valence [$n_{Cl}+\sigma^*_{CH}$] character (see Table III). The predicted oscillator strength is very weak. At both DFT and TDDFT (M06-2X) levels the optimized geometry of the 1^1B_1 state in the C_{2v} point group corresponds, however, to a transition state whose vibrational wavenumbers have been calculated (see Table IV). As discussed in Section IV B, optimization attempts in lower symmetry groups were unsuccessful. The identified peaks of the very weak signal are shown by dashed lines in Fig. 5b. An average separation of 0.12±0.01 eV (960±80 cm^{-1}) could be determined. This compares favorably with the values of 933 cm^{-1} (TDDFT) or 944 cm^{-1} (DFT) predicted for the in-plane C-H bending mode excitation ν_3 (see Fig. 3) and is compatible with the large change in the optimized H-CC angle (see Table S1).

The 6.0-7.0 eV energy range consists of a complex series of fairly narrow peaks entangled in a sequence of broader structures. As far as the diffuse features starting at 6.16 eV are concerned, a regularly distributed intensity is observed up to 7.0 eV at intervals of about 0.15±0.02 eV (1200±160 cm^{-1}). The maximum intensity for this progression is observed at 6.62 eV. The most probable transition at this energy is likely the $\pi\rightarrow\pi^*(3^1B_2)$ transition whose vertical energy is predicted at 6.55 eV at the TDDFT level (see Table III). As mentioned in Section IV B, this state has to cross the ground state, leading to an internal relaxation which may be responsible for the diffuseness of the detected structures. Arulmozhiraja et al.[14] calculated this excitation at 6.93 eV. The vibrational structure with $\omega\approx1200\pm160$ cm^{-1}, superimposed on the strong continuum may likely be assigned to the ν_2(C=C stretching) or ν_3(C-H bending) vibrations (see Fig. 3) calculated at 1269 cm^{-1} and 1112 cm^{-1} respectively (see Table IV). The large change in the C=C bond length of the optimized geometry of the 3^1B_2 state (Table S1) is expected to induce an excitation of the C=C stretching vibration.

Fig. 4 compares the relative energy position of these two transitions in chlorinated compounds: C_2H_4 is used as a reference. Fig. 4a shows that the presence of a second Cl-atom induces a shift to lower energy of the σ^* and π^* states. For the latter a systematic energy lowering from 6.880 eV (C_2H_3Cl)[37] to 6.620 eV (cis-1,2-$C_2H_2Cl_2$) and 6.482 eV (1,1-$C_2H_2Cl_2$)[16] is observed. The substitution in cis-position induces a shift to higher energy with respect to the 1,1-isomer. Fig. 4b clearly shows the expected shift to lower energy produced by the substitution of F by a Cl-atom in the cis-isomers: from 7.11 eV[38] to 6.62 eV.

The short sequence of narrower peaks observed between 6.4 eV and 7.0 eV and assigned to the $\pi(2b_1)\rightarrow$3s Rydberg transition will be discussed in the next section V B 1.

Above the photon energy of 7.0 eV, several valence transitions are predicted by quantum chemical calculations,

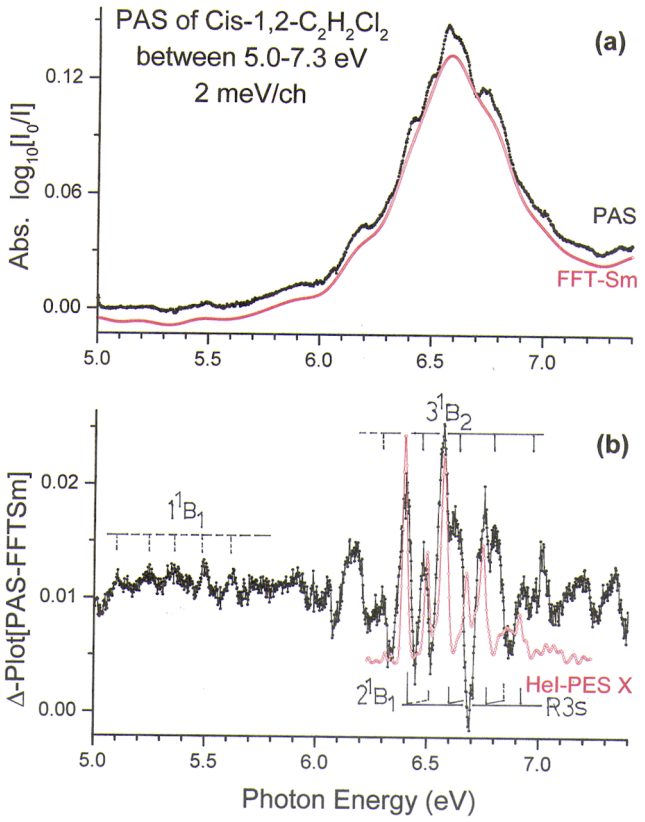

FIG. 5. (a) Vacuum UV photoabsorption spectrum of cis-1,2-$C_2H_2Cl_2$ on an expanded. photon energy scale between 5.0 eV and 7.5 eV. The continuous red curve labeled FFT-Sm corresponds to the strongly smoothed PAS curve by fast Fourier transform. (b) Δ-plot of the PAS. Vertical bars indicate the vibrational progressions. The red curve corresponds to the HeI-PES band of the $\tilde{X}^2B_1$ cationic state of cis-1,2-$C_2H_2Cl_2$.

i.e. at 7.32 eV, 8.58 eV and 9.15 eV successively (see Table III). In agreement with these predictions, a short but fairly well defined progression consisting of three broad weak peaks starts at 7.322 eV (see Fig. 1) and is followed by structures at 7.477 eV and at 7.613 eV (see Fig. 6a). These structures are superimposed on a broad background with its maximum at 7.6 eV (see red curve in Fig. 1). We suggest to assign this part of the spectrum to the $n_{Cl}+\sigma_{CH}\rightarrow\pi^*$ transition predicted at 7.32 eV and leading to the 5^1B_1 state (see Table III). The average interval of 0.146±0.009 eV (1180±70 cm^{-1}) could be assigned to the excitation of the C-H bending vibration (see Fig. 3 and Table IV). This assignment is also supported by the predicted geometry changes in the optimized conformation (see Table S1). Mahncke and Noyes[10] mentioned non-assigned "diffuse bands" at 60562 cm^{-1} (7.509 eV) and 61169 cm^{-1} (7.583 eV) which are probably related to the present observations.

Below and close to the first vertical ionization limit of cis-1,2-$C_2H_2Cl_2$ at 9.843 eV,[23] two additional broad structure are observed, with maxima at 8.5 eV and 9.8 eV (see red curve in Fig. 1). They may correlate with the transition energies predicted at the TDDFT level for $n_{pz,Cl}+\pi_{CCl}\rightarrow\pi^*$ at 8.58 eV (14^1A_1) and $n_{Cl}+\sigma_{CC}+\sigma_{CH}\rightarrow\pi^*$ at 9.15 eV (20^1B_2) respectively (see Table III). For comparison, Arulmozhiraja et al.[14] calculated seven valence as well as Rydberg transitions taking place between 8.04 eV and 8.43 eV: the lowest $n\rightarrow\pi^*$ excitation is at 8.04 eV whereas two $n\rightarrow\sigma^*$ transitions were predicted at 8.24 eV and 8.38 eV. It is thus likely that both valence and Rydberg states are implied in this region of the absorption spectrum and the fine structure superimposed on the broad background might be interpreted as resulting from transitions to Rydberg states as discussed in the next section.

B. The Rydberg transitions

In Fig. 1 the PAS of cis-1,2-$C_2H_2Cl_2$ measured in the photon energy range of 7.0 eV to about 13.0 eV displays numerous structures of variable intensity. Particularly from 7.4 eV up to about 9.0 eV, it exhibits a series of weak to very weak sharp features besides one stronger and broad transition. The original spectrum and the corresponding Δ-plot are displayed on an expanded energy scale in Fig. 6(a–d) for the 7.0-13.0 eV range. Between 7.0 and 10.0 eV, the spectrum has been recorded with 500 μeV energy increments.

As no prior information on the coupling among Rydberg states is available for this molecule, we used the Rydberg formula (1) as a zero-order assumption for the assignment of the spectral transitions:

$$E_{Ryd} = IE - R/(n-\delta)^2 = IE - R/(n^*)^2 \quad (1)$$

In (1), R=13.6057 eV[24] is the Rydberg constant, δ is the quantum defect, and IE represents the ionization energy corresponding to the ionic state to which the Rydberg series converges. Any significant Rydberg-Rydberg coupling is then expected to affect the quality of the fits of the Rydberg formula to the experimental data. Furthermore, in the absence of coupling between Rydberg series, the quantum defect δ has typical values which are characteristic of the angular momentum of the Rydberg orbital. When couplings are involved, these values may be perturbed. Such perturbations already allowed us to identify and quantitatively analyze transition between Hund's coupling cases.[39] The quantum defect values are therefore important parameters to be determined.

The observed intensity distributions of the spectral features show Franck-Condon-like behaviors and do not follow the n^{-3} law, so that vibrational excitation of the successive Rydberg states dominates the spectrum. If Rydberg-Rydberg couplings may be neglected, it is sensible to assume that very similar potential energy surfaces characterize the Rydberg states and the ionic state to which they converge, so that similar vibrational structures are expected for a Rydberg state and the corresponding ionic state.[38] The quality of the fits indicates *a posteriori* whether this assumption holds. This procedure has already been successful to disentangle the vibrational structure in the vacuum UV spectra of C_2H_3F,[40] 1,1-$C_2H_2F_2$[41]

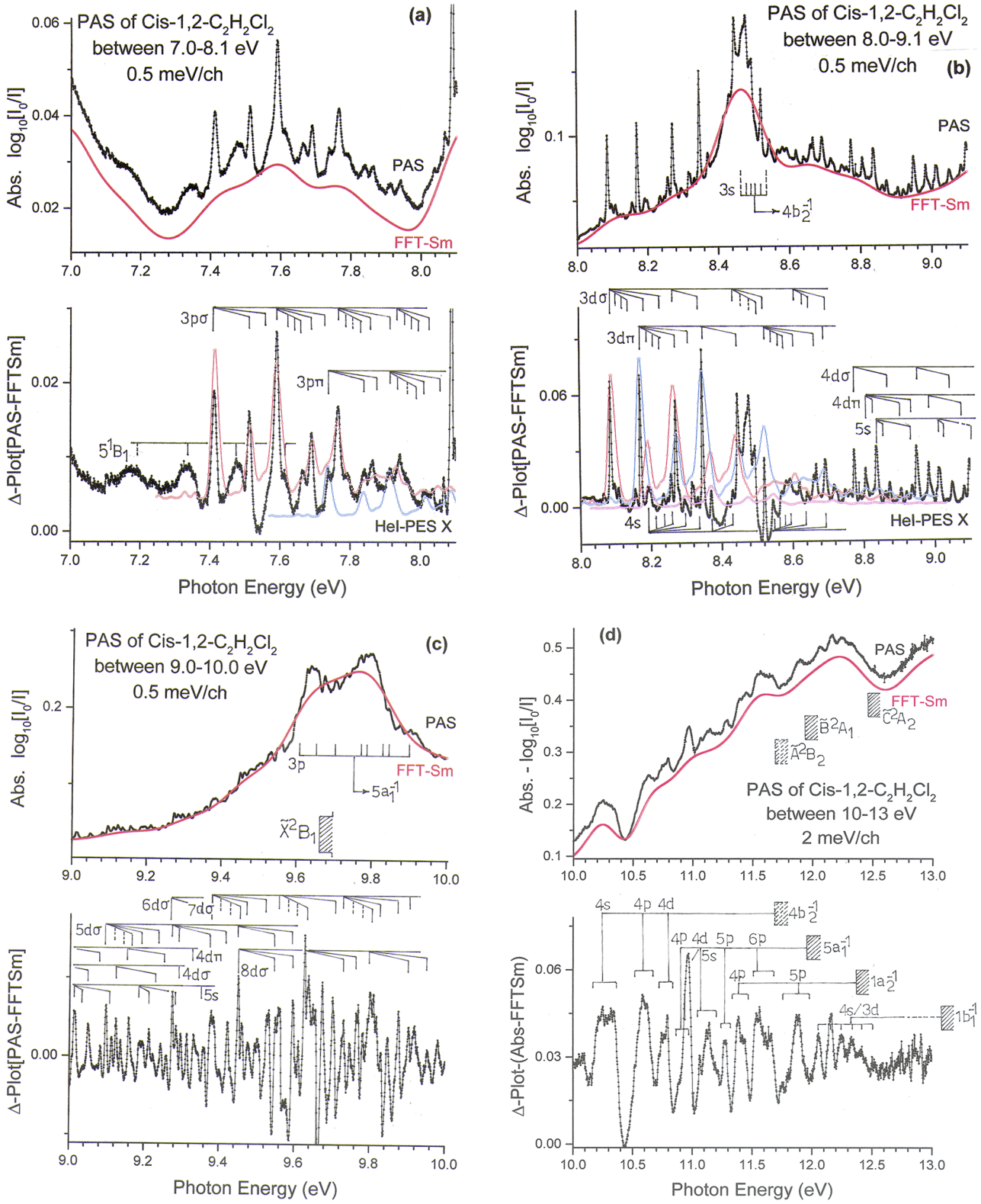

FIG. 6. Vacuum UV photoabsorption spectrum of cis-1,2-$C_2H_2Cl_2$ on an expanded. photon energy scale between 7.0 eV and 13.0 eV. The upper and lower parts show the absorbance and the corresponding Δ-plot respectively for (a) 7.0-8.1 eV, (b) 8.0-9.1 eV, (c) 9.0-10.0 eV and (d) 10.0-13.0 eV. Vibrationless (0,0) transitions are indicated as long vertical bars, whereas the vibrational progressions are indicated as short bars. The $\tilde{X}^2B_1$-HeI-PES band is inserted by red, blue and magenta open dots. The $1b_1^{-1}$ continuum lies at 13.592 eV.

and 1,1-C_2H_2FCl.[42] In the present case, to make the comparison easier, the Δ-plot of the appropriate PAS energy range will be compared to the HeI-PES of the cis-1,2-$C_2H_2Cl_2^+$ in its ground or excited states as measured in our laboratory.[23]

1. Vibrationless Rydberg transitions between 6.4 eV and 10 eV (see Fig. 1)

The vibrationless Rydberg transitions observed for cis-1,2-$C_2H_2Cl_2$ and converging to the first ionization limit lie between 6.4 eV and 9.7 eV and are labeled in Fig. 1. Table I lists the energies and wavenumbers of these transitions with their associated effective quantum numbers and compares the results of the present work with previous investigations by Mahncke and Noyes,[10] Walsh[11] and Walsh and Warsop.[12] The assignments are based on an adiabatic ionization energy for the ionic ground state equal to 9.666±0.006 eV,[23] in good agreement with the value provided by Walsh and Warsop (IE = 9.652 eV).[12] As mentioned in section II, the estimated uncertainty on the transition energies is 2 meV (16 cm^{-1}). No error estimation is available for the literature data.[10–12]

The observed $\pi(2b_1)\rightarrow$ns Rydberg series converging to the first ionization energy limit are listed in Table I. The average quantum defect over the n=3 to 8 range is equal to $\bar{\delta}$= 0.96±0.01. By quantum chemical calculation at the TDDFT level, the lowest $\pi\rightarrow$R's'(2^1B_1) vertical transition energy is equal to 6.35 eV (see Table III), in good agreement with the present experimental value at 6.398 eV.

Mahncke and Noyes[10] identified a Rydberg series converging to 78103 cm^{-1} (9.683 eV) with δ=0.01 but the first member of the series was missing, hidden in the 1850 Å (6.70 eV or 54 054 cm^{-1}) continuum. So did Walsh[11] who determined the convergence limit at 77937 cm^{-1} (9.663 eV) with δ=0.05: the first member also failed. Walsh and Warsop[12] reported a Rydberg series starting at 65182 cm^{-1} (8.082 eV) converging to 77850 cm^{-1} (9.652 eV) with δ=0.93.

Transitions from the $\pi(2b_1)$ to np Rydberg orbitals lead to two well-identified series (Table I), as was also observed in previous studies on 1,1-$C_2H_2Cl_2$,[16] 1,1-$C_2H_2F_2$,[41] 1,1-C_2H_2FCl,[42] and CH_3X (X=Cl, Br and I).[39] The two series are observed up to n=8. We assign the series starting at 7.414 eV to the $\pi(2b_1)\rightarrow$npσ transitions whereas the series starting at 7.740 eV is assigned to $\pi(2b_1)\rightarrow$npπ. These assignments are based on the good agreement with the theoretical predictions of the present work listed in Table III: $\pi\rightarrow$Rpσ (8^1B_1) and $\pi\rightarrow$Rpπ (11^1A_1) transitions were calculated at 7.44 eV and 7.90 eV successively. Both transitions have noticeable oscillator strength. The splitting of 0.326 eV between the two 3pλ -type states is very close to the value of 0.356 eV observed in 1,1-$C_2H_2Cl_2$.[16] In 1,1-$C_2H_2F_2$, however, the splitting is substantially smaller (0.183 eV),[41] while it is again of the same order of magnitude in 1,1-C_2H_2FCl (0.404 eV).[38,42]

Average quantum defects $\bar{\delta}$=0.53±0.01 and 0.34±0.02 are determined for the npσ- and the npπ-type Rydberg series respectively. The small dispersion of the quantum defects along the series is compatible with our assumed neglect of the Rydberg-Rydberg couplings. The difference between the quantum defects for the npσ- and the npπ series can be interpreted as follows. The presence of more σ orbitals than π orbitals in the ionic core leads to a stronger core-Rydberg interaction for σ-type Rydberg orbitals, so that a larger quantum defect should be observed for npσ compared to npπ Rydberg orbitals. In the C_{2v} point group, the npσ and npπ orbitals should rigorously be denoted by npa_2 and npb_1. However, assuming the molecular ion field to be nearly cylindrical (diatomic-like), the σ, π, ... nomenclature is usually used.

A first $\pi(2b_1)\rightarrow$ndλ series starts at 8.089 eV and its members are characterized by an average quantum defect $\bar{\delta}$=0.08±0.03. The second series starting at 8.170 eV is characterized by an average quantum defect $\bar{\delta}$= 0.002±0.008. These $\bar{\delta}$ values suggest ndσ and ndπ Rydberg states respectively. In the vacuum UV spectrum of 1,1-$C_2H_2F_2$[41] and of 1,1-C_2H_2FCl,[38,42] a ndσ series is observed with $\bar{\delta}$=0.13±0.03[41] and 0.125±0.025[41] respectively. For the corresponding ndπ series $\bar{\delta}$=0.04±0.03[40] and $\bar{\delta}$=-0.11±0.02[41] were respectively determined. Surprisingly, the splitting between 3dσ and 3dπ is found to be equal to 0.081 eV in cis-1,2-$C_2H_2Cl_2$, although it is much greater, 0.214 eV, in 1,1-C_2H_2FCl[42] and 0.109 eV in 1,1-$C_2H_2F_2$.[41]

Finally, a fairly strong broad and complex structured band is observed at about 8.5 eV, as already mentioned in Section V A, where the broad signal is interpreted as resulting from a valence-valence $n_{pz,Cl}+\pi_{CCl}\rightarrow\pi^*$ transition. Superimposed fine structure is observed, however, whose energy positions are listed in Table VI. In the densitometer trace of the PAS published by Walsh and Warsop[12] a strong broad and roughly structured band is observed at 68 310 cm^{-1} (8.469 eV) showing several shoulders between 67 294 cm^{-1} (8.343 eV) and 68697 cm^{-1} (8.517 eV) but these structures were not discussed or assigned by the authors. The structures reported in Table VI, with an adiabatic excitation energy of 8.446 eV, do not fit into the possible Rydberg series converging to the ground ionic state and which have been detailed above. Based on our quantum chemical TDDFT computations (Table III), which predict the vertical $(4b_2{:}n_{Cl}+\sigma_{CH})\rightarrow$3s transition at 8.24 eV, we rather suggest to assign the structures starting at 8.446 eV to transitions to the vibrational levels of the lowest Rydberg state (3s) converging to the$\tilde{A}^2B_2$ ionic state, whose vertical

TABLE VI. Energy positions (eV), wavenumbers (cm^{-1}) and effective quantum numbers associated with the structures in the strong broad band observed at 8.5 eV in the vacuum UV-PAS of cis-1,2-$C_2H_2Cl_2$. Conversion factor: 1 eV= 8065.545 cm^{-1}.[24]

eV	cm^{-1}	n^*	Assignment
8.446	68121	2.050	$n_{Cl}+\sigma_{CH}\rightarrow$3s converging to $\tilde{A}^2B_2$
8.478	68380	2.044	
8.495	68517	2.038	
8.503	68565	2.034	
8.521	68726	2.030	
8.544	68912	2.026	

ionization energy is equal to 11.690 eV.[23] Based on the information from the photoelectron spectrum,[23] we infer n^*=2.05±0.01 or δ=0.95±0.01, which is perfectly compatible with a 3s Rydberg state.

2. Vibrational analysis (Fig. 3, Fig. 5 and Fig. 6(a–c))

After having identified the vibrationless Rydberg transitions, the vibrational structure of the identified electronic states has to be disentangled. To this purpose we will rely on the assumption stated above, i.e. the vibrational structure of the Rydberg states should be close to that of the cationic states to which they converge.[39] This information will be inferred from the HeI-PES.[23] A comparison between the PAS and the HeI-PES of the ground state of the cation is illustrated in Fig. 5, Figs. 6a and 6b. Most of the Rydberg states observed between 6.4 eV and 9.9 eV converge to $IE_{ad}(\tilde{X}^2B_1)$ = (9.666±0.006) eV of cis-1,2-$C_2H_2Cl_2$.[23] The electronic ground state of the cation mainly shows three vibrational modes:[23,32] ω_2^+=1460±30 cm^{-1} (181±4 meV), ω_3^+=1160±20 cm^{-1} (144±3 meV) and ω_4^+=860±60 cm^{-1} (107±8 meV). These values correspond to the C=C stretching, C-H in-plane bending and C-Cl stretching vibrations respectively.

The first Rydberg transition $2b_1(\pi)\rightarrow R3s(2^1B_1)$ with an adiabatic excitation energy of 6.398 eV (see Fig. 5) shows vibrational excitation at 6.568 eV (v=1), 6.752 eV (v=2) and 6.930 eV (v=3). The average wavenumber $\bar{\omega}$= 1420±70 cm^{-1} (176±9 meV) corresponds to ν_2 (C=C stretching) predicted at 1427 cm^{-1} (see Table IV). Excitations corresponding to smaller wavenumbers (short dashed vertical lines in Fig. 5) are likely hidden in the signal corresponding to the 3^1B_2 valence excited state.

The application of the same procedure is displayed in Fig. 6(a–c). Table S2(a-c) reports the transition energies and the proposed corresponding assignments.

The 7.4-8.1 eV photon energy range shows weak broad bands alternating with stronger sharp peaks. The broad weak features have already been assigned earlier in this work (see section V A). The sharper features are assigned to the $2b_1\rightarrow 3p\sigma$ and $2b_1\rightarrow 3p\pi$ Rydberg transitions with adiabatic excitation energies at 7.414 eV and 7.740 eV respectively (see section V B 1 and Table I). Both states show an extended vibrational structure as analyzed in Table S1a and illustrated in Fig. 6a. Energy positions in square brackets indicate that at least two different assignments are possible and that these should be considered with caution. Intensity fluctuations may result from the overlap of several contributions. At least two vibrational modes are excited in both states, i.e. ω=1420±20 cm^{-1} (176±2 meV) and ω'=795±15 cm^{-1} (98±2 meV). In addition, two weaker modes are detected with wavenumbers of 1220±20 cm^{-1} (151±3 meV) and of 190±30 cm^{-1} (24±4 meV).

Their assignment relies on the comparison with the ground state cation. The first two wavenumbers should correspond to ω_2^+(C=C stretch)= 1430±30 cm^{-1} and to ω_4^+(C-Cl symmetric stretch)= 860±60 cm^{-1} respectively.[23,32] The latter value is significantly higher in the cation than in the Rydberg state. However, this result agrees with the quantum chemical calculations performed on the two systems[23] and in the present work: for the Rydberg excitation only the C=C stretching is significantly modified whereas the C-Cl stretching remains only slightly affected in most of the excited neutral states (e.g. see Table IV).

The wavenumber equal to 1220±20 cm^{-1} can be correlated with the value of 1160±20 cm^{-1} inferred from the HeI-PES for the ground state cation. This vibration corresponds to ν_3 (C-H bending) predicted at 1215 cm^{-1} by ab initio calculations.[23] The wavenumber of 190±30 cm^{-1} is not detected in the HeI-PES. An assignment to ν_5 (C-Cl bending) is proposed based on quantum chemical predictions (193 cm^{-1}).[23] However, as mentioned in Table S2a, ω_3 is close to $\omega_4+2\omega_5$ which introduce ambiguities in the assignments.

Table S2a also compares the present results to those reported by Walsh and Warsop[12] (see Table S2a, col. 6). These authors proposed a classification of the bands and determined two wavenumbers, i.e. of about 1400 cm^{-1} and 800 cm^{-1}. The comparison of Table VIIa with Table I in Ref. 12 shows a very good agreement and the present work brings a strong argument supporting the assignments. These authors also mentioned a wave number of 1224 cm^{-1} but rejected it because "...no frequency of this magnitude is observed *in any other electronic transition of cis-dichloro ethylene* or in the transitions of the other chloroethylenes". As mentioned above, this wavenumber is very probably involved in both the two 3pσ and 3pπ Rydberg states and very likely in combinations in the 3pσ Rydberg state.

Fig. 6b shows the PAS in the 8.0-9.1 eV range on an expanded energy scale. This part of the spectrum is much more crowded and the energy positions of the features are listed in Table S2b. The procedure described earlier in this section (HeI-PES inserted in Fig. 6b) leads to the assignments presented in the same table.

At least seven Rydberg transitions are observed. Six of them converge to the ground state of the cation and correspond to $2b_1\rightarrow 3d\sigma$, $3d\pi$, 4s, $4d\sigma$, $4d\pi$ and 5s successively. The strong broad peak around 8.5 eV has already been interpreted as a superposition of a valence-valence ($n_{pz,Cl}+\pi_{CCl}\rightarrow\pi^*$) and a valence-Rydberg ($4b_2\rightarrow 3s$) transition. (see section V B 1).

For the six Rydberg states, the vibrational analysis leads to four vibrational wavenumbers: ω_2=1426±9 cm^{-1} (177±1 meV), ω_3=1180±20 cm^{-1} (146±2 meV), ω_4=806±7 cm^{-1} (100±1 meV) and ω_5=191±8 cm^{-1} (24±1 meV). These values are close to those already mentioned for the 3pσ and 3pπ states. We notice that ω_3 is slightly lower and closer to the value ω_3^+=1160±20 cm^{-1} of the cation ground state.[23]

In Table S2b the assignments proposed in the present work are compared to the classifications attempted by Walsh and Warsop.[12] These authors proposed two possible interpretations of the bands observed between 65000-69000 cm^{-1}, assigned either to $2b_1\rightarrow 3d\sigma$ or to $2b_1\rightarrow 3d\pi(\delta)$ Rydberg

transitions. Three wavenumbers arose from their analysis at 1424 cm^{-1}, 813 cm^{-1} and 197 cm^{-1}. These three values are in good agreement with the present results. However, they did not detect the wavenumber at 1177 cm^{-1} observed in the present work.

Fig. 6c shows the 9.0-10.0 eV energy range on an expanded scale. A large number of weak to very weak structures as well as broad intense peaks at about 9.6 eV and 9.8 eV are observed. The Δ-plot shown in the lower panel of Fig. 6c enhances these structures. Their energy positions and the proposed assignments in terms of transitions to vibrationally excited Rydberg states converging to the ionic ground state are listed in Table S2c. The majority of the observed transitions are interpreted as leading to ndσ (n=5-8) Rydberg states. As expected, the same vibrational normal modes are involved as for the previous series. The average wavenumbers are ω_2=1411±8 cm^{-1} (175±1 meV), ω_3=1170±20 cm^{-1} (145±3 meV), ω_4=807±20 cm^{-1} (100±2 meV) and ω_5=190±20 cm^{-1} (24±2 meV). The present energy range being almost outside the prospected region of previous photoabsorption works,[10-12] no comparison can be made. Only Mahncke and Noyes[10] mentioned a few discrete bands which have been introduced in Table S2c. Most of them fit the present data and possible assignments are proposed.

We could not observe any significant breakdown of the Rydberg formula or of the assumption of similar vibrational structures for the Rydberg states and the corresponding cationic state. This suggests that Rydberg-Rydberg or Rydberg-continuum interactions are too small to affect the energy positions at the resolution and accuracy reached in our spectra.

Beside the long sequence of weak structures, the present region also shows a strong complex structured doublet peak spread between 9.6 eV and 9.9 eV (see Fig. 1 and Fig. 6c, upper panel). The steep absorbance increase is likely linked to the opening of the $2b_1^{-1}$ ionization continuum at 9.666 eV. Rydberg states converging to higher lying ionization limits need to be considered. As shown in Fig. 1, three ionization continua are open between 11.5 eV and 12.2 eV, i.e. $4b_2^{-1}$ at 11.426 eV, $5a_1^{-1}$ at 11.965 eV and $1a_2^{-1}$ at 12.375 eV.[23,32-34]

Based on the vibrational structure of the $\tilde{B}^2A_1$ photoelectron band,[23] the unassigned features observed in the 9.6-9.9 eV range could be interpreted (see Table VII and upper panel of Fig. 6c). The effective quantum number n^*=2.426±0.005, averaged over eight vibronic transitions, suggests an assignment to a $5a_1 \rightarrow 3p$ Rydberg transition.

3. Rydberg transitions between 10 eV and 20.0 eV (see Figs. 1, 2, (6)d)

The PAS of cis-1,2-$C_2H_2Cl_2$ between 10 eV and 13 eV has been recorded with 2 meV increments and is reproduced in Fig. 6d. The absorbance steadily increases over the whole range. It shows a sequence of weak broad bands. Several of these features are clearly consisting of very weak substructures. They become more apparent in the Δ-plot (lower panel in Fig. 6d) and show intervals of the order of 30 meV (240 cm^{-1}). To try to disentangle this range of the PAS it would be reasonable to use the same hypotheses and assumptions applied earlier. Using the present data, term values and effective quantum numbers could be derived.

TABLE VII. Analysis of the high energy bands observed in the vacuum UV photoab- sorption spectrum of cis-1,2-$C_2H_2Cl_2$. Energy positions (eV), corresponding wavenumbers (cm^{-1}), effective quantum numbers (n^*) and assignments as proposed in this work. Conversion factor: 1 eV= 8065.545 eV.[24]

Energy Position (eV)	(cm^{-1})	n^*	Assignment
Rydberg Series converging to $IE_{ad}(\tilde{B}^2A_1)$=11.965 eV[23] $5a_1 \rightarrow 3p$ (n^*_{av}=2.43±0.01)			
9.648	77816	2.423	
9.718	78381	2.429	
9.768	78784	2.438	
9.781	78889	2.423	
9.829	79276	2.426	
9.854	79478	2.423	
9.901	79857	2.426	
Rydberg Series converging to $IE_{ad}(\tilde{D}^2B_1)$=13.592 eV[23] $1b_1 \rightarrow 4s/3d$ (n^*_{av}=3.00±0.02)			
12.054	97222	2.974	$hc\omega_{av}$ =90±8 meV or 720±30 cm^{-1}
12.152	98012	3.002	
12.248	98787	3.012	
12.328	99432	3.009	
12.412	100110	3.028	

In this energy range three vertical ionization limits, lying close together, are involved, i.e. 11.690 eV ($4b_2^{-1}$), 12.028 eV ($5a_1^{-1}$), and 12.460 eV ($1a_2^{-1}$)[23,32-34] successively. They are inserted in Fig. 6d (upper panel). The sum of the associated continua contributes to the strong increase of the background observed in the PAS in this energy range. All three cationic states are characterized by an extended vibrational progression.[23]

If we assume that the maxima at 10.252 eV, 10.584 eV and 10.792 eV (Table II) correspond to transitions to Rydberg states converging to the $4b_2^{-1}$ continuum at 11.69 eV, effective quantum numbers of 3.08, 3.51 and 3.89 are respectively obtained. This is compatible with $4b_2 \rightarrow$ 4s, 4p and 4d assignments (Figure 6d).

The next four well identified bands lye at 10.880 eV, 11.120 eV, 11.275 eV and 11.536 eV (Table II). Based on their effective quantum numbers n^*=3.44, 3.87, 4.25 and 5.25, they may be assigned to $5a_1 \rightarrow$ 4p, 4d (or 5s), 5p and 6p transitions, respectively. The last two bands at 11.342 eV and 11.75 eV will be assigned to $1a_2 \rightarrow$ 4p and 5p transitions for which effective quantum numbers $n*$=3.49 and 4.38 are obtained. The substructures detected in these bands could likely be assigned to vibrational excitations, e.g. of C-Cl bending for which a wave number of the order of 180 to 270 cm^{-1} has been predicted for several Rydberg and valence states (see Table IV) and cationic states as well.[23]

The width of all these bands has likely to be related to the short lifetimes of these Rydberg states. In a forthcoming paper[23] it will be shown that these Rydberg states mainly undergo resonant autoionization to the ionic ground state of cis-1,2-$C_2H_2Cl_2^+(\tilde{X}^2B_1)$ giving rise to threshold photoelectrons.

A broad band spreads from 12.054 eV to 12.412 eV and consists of five narrower well resolved regularly spaced features with a regular intensity distribution. Assuming the $\tilde{D}^2B_1$ state of the cation at 13.592 eV as convergence limit[23] (see Table VII) an average effective quantum number $n^*=3.00\pm0.02$ is obtained. Therefore, this band is tentatively ascribed to a $1b_1\rightarrow4s/3d$ Rydberg transition. The vibrational analysis leads to an averaged wavenumber $\bar{\omega}= 722\pm30$ cm^{-1} which could likely be assigned to ν_4 (C-Cl stretch/C-H bending) as predicted for other lower lying neutral excited states (see Table IV).

The energy range between 13 eV and 20 eV has been recorded with the 1.5m-NIM monochromator and with 15 meV energy increments. This high energy range only shows a few very broad bands superimposed on a slower increasing continuum as shown in Fig. 2a. The band maxima are listed in Table II. In the same energy range five ionic excited states are observed in the HeI PES, i.e. at 13.592 ($1b_1^{-1}$), 14.083 eV ($3b_2^{-1}$), 15.531 eV ($4a_1^{-1}$), 16.638 eV ($3a_1^{-1}$) and at 18.84 eV ($2b_2^{-1}$) successively.[23,32–34]

In Fig. 2b the Δ-plot has been reproduced and slightly smoothed by FFT to increase the signal/noise ratio. At least six broad bands are characterized by a full width half-maximum (FWHM) ranging from 0.4 eV to 0.7 eV. A last very broad band extends from 16.8 eV to 19.5 eV. The energy position of the successive maxima is listed in Table II. A tentative classification based on the vertical ionization energies and the inferred effective quantum numbers is also provided in Table II.

VI. CONCLUSIONS

The measurement of the VUV photoabsorption spectrum of cis-1,2-$C_2H_2Cl_2$ at higher resolution by using synchrotron radiation enabled us to extend the data above the 10.5 eV photon energy limit and, for the first time, up to 20 eV. In this energy range the absorbance drastically increases and numerous bands are identified. Interpretations and assignments have been proposed.

Quantum chemical calculations allowed us to describe and assign valence-valence ($2b_1(\pi)\rightarrow\sigma^*/\pi^*$) as well as valence-Rydberg ($2b_1(\pi)\rightarrow3s$) transitions which are involved at the low energy end of the spectrum, i.e. between 5 eV and 7.4 eV. Below 6.0 eV the 1^1B_1 state has a strongly mixed valence ($n_{Cl}+\sigma^*_{CH}$)/Rydberg (Rpσ) character. Above 6.0 eV the $\pi\rightarrow\pi^*$ (3^1B_2) valence and the $\pi\rightarrow3s$ (2^1B_1) Rydberg transitions are entangled. For the vibrational structure of both states an assignment is proposed. Above 7.0 eV several valence transitions are predicted by the calculations and compared to the observations.

In the intermediate photon energy range, i.e. between 6.4 eV and 10.0 eV, a large number of narrow vibronic Rydberg transitions, i.e., $2b_1\rightarrow ns$ (n=3-8), two types of np (up to n=8) and two nd-type (up to n=9) series, have been identified and interpreted. The involved Rydberg states converge to the cis-1,2-$C_2H_2Cl_2^+(\tilde{X}^2B_1)$ ground ionic state. By reference to the first band of the cis-1,2-$C_2H_2Cl_2$ HeI-PES,[23] the vibrational structure has been assigned to four vibrational modes, including harmonics and combinations: $\omega_2 \approx 1420$ cm^{-1} (C=C stretching), $\omega_3 \approx 1190$ cm^{-1} (C-H symmetric bending), $\omega_4 \approx 800$ cm^{-1} (C-Cl symmetric stretching) and $\omega_5 \approx 190$ cm^{-1} (C-Cl symmetric bending). These assignments are compared to those proposed on a more empirical basis in previous reports.[11,12]

At 8.5 eV, 9.6 eV and above 10.0 eV numerous Rydberg transitions are observed, all assigned to members of series converging to the successive excited states of cis-1,2-$C_2H_2Cl_2^+$. For a few of them vibrational progressions are observed.

SUPPLEMENTARY MATERIAL

See supplementary material for the optimized geometry parameters of neutral ground and excited states of cis-1,2-$C_2H_2Cl_2$ (Table S1) and the list of the vacuum UV spectral features measured between 7.41 eV and 9.94 eV (Table S2).

ACKNOWLEDGMENTS

Financial supports by the European Commission, the University of Liège and the Belgian program on Interuniversity Attraction Poles of the Belgian Science Policy (IAP no. P6/19) are gratefully acknowledged.

REFERENCES

[1] L. J. Carpenter and S. Reimann (Coordinating Lead Authors), Ozone-Depleting Substances (ODSs) and other Gases in the Montreal Protocol, Chapter 1, pp 1.50 in *Scientific Assessment of Ozone Depletion*: 2014, Global Ozone Research and Monitoring Project–Report No. 55, World Meteorological Organization, Geneva, Switzerland.
[2] K. Kirchner, D. Helf, P. Ott, and S. Vogt, Ber. Bunsen-Ges. Phys. Chem. **94**, 77 (1990).
[3] S. Ramamoorthy, *Chlorinated Organic Compounds in the Environment. Regulatory and Monitoring Assesment* (Lewis Publishers, Boca Raton, Fl (USA), 1998).
[4] M. J. Berry, J. Chem. Phys. **61**, 3114 (1974).
[5] M. Umemoto, K. Seki, H. Shinohara, U. Nagashima, N. Nishi, M. Kinoshita, and R. Shimada, J. Chem. Phys. **83**, 1657 (1985).
[6] M. Chandra, D. Senapati, M. Tak, and P. K. Das, Chem. Phys. Letters **430**, 32 (2006).
[7] T. Yamada, A. El-Sinawi, M. Siraj, P. H. Taylor, J. Peng, X. Hu, and P. Marshall, J. Phys. Chem A **105**, 7588 (2001).
[8] C. E. Canosa-Mas, T. J. Dillon, H. Sidebottom, K. C. Thompson, and R. P. Wayne, Phys. Chem. Chem. Phys **3**, 542 (2001).
[9] V. A. Mikhailov, M. A. Parkes, R. P. Tuckett, and C. A. Mayhew, J. Phys. Chem. A **110**, 5760 (2006).
[10] H. E. Mahncke and W. A. Noyes, Jr., J. Chem. Phys. **3**, 536 (1935).
[11] A. D. Walsh, Trans. Faraday Soc. **41**, 35 (1945).
[12] A. D. Walsh and P. A. Warsop, Trans. Faraday Soc. **64**, 1418 (1968).

[13]C. F. Koerting, K. N. Walzl, and A. Kuppermann, Chem. Phys. Letters **109**, 140 (1984).
[14]S. Arulmozhiraja, M. Ehara, and H. Nakatsuji, J. Chem. Phys. **129**, 174506 (2008).
[15]O. G. Khvostenko, J. Electr. Spectr. Rel. Phenomena **195**, 220 (2014).
[16]R. Locht, D. Dehareng, and B. Leyh, J. Phys. Commun. **1**, 045013 (2017).
[17]R. Locht, D. Dehareng, and B. Leyh, unpublished results.
[18]A. Hoxha, R. Locht, B. Leyh, D. Dehareng, H.-W. Jochims, and H. Baumgärtel, Chem. Phys. **256**, 239 (2000).
[19]R. Locht, B. Leyh, A. Hoxha, D. Dehareng, H.-W. Jochims, and H. Baumgârtel, Chem. Phys. **257**, 283 (2000).
[20]R. Locht, D. Dehareng, and B. Leyh, J. Phys. B At. Mol. Opt. Phys. **47**, 085101 (2014).
[21]P. Marmet, Rev. Sci. Instrum. **50**, 79 (1979); R. Carbonneau, E. Bolduc, and P. Marmet, Can. J. Phys. **51**, 505 (1973).
[22]R. Carbonneau and P. Marmet, Can. J. Phys. **51**, 2203 (1973); Phys. Rev. A **9**, 1898 (1974).
[23]R. Locht, D. Dehareng, and B. Leyh, unpublished results.
[24]P. J. Mohr, B. N. Taylor, and D. B. Newell, J. Phys. Chem. Ref. Data **45**, 043102 (2016); P. J. Mohr, D. B. Newell, and N. B. Taylor, Rev. Mod. Phys. **88**, 035009 (2016).
[25]M. J. Frisch, G. W. Trucks, H. B. Schlegel, G. E. Scuseria, M. A. Robb, J. R. Cheeseman, G. Scalmani, V. Barone, B. Mennucci, G. A. Petersson, H. Nakatsuji, M. Caricato, X. Li, H. P. Hratchian, A. F. Izmaylov, J. Bloino, G. Zheng, J. L. Sonnenberg, M. Hada, M. Ehara, K. Toyota, R. Fukuda, J. Hasegawa, M. Ishida, T. Nakajima, Y. Honda, O. Kitao, H. Nakai, T. Vreven, J. A. Montgomery, Jr., J. E. Peralta, F. Ogliaro, M. Bearpark, J. J. Heyd, E. Brothers, K. N. Kudin, V. N. Staroverov, R. Kobayashi, J. Normand, K. Raghavachari, A. Rendell, J. C. Burant, S. S. Iyengar, J. Tomasi, M. Cossi, N. Rega, J. M. Millam, M. Klene, J. E. Knox, J. B. Cross, V. Bakken, C. Adamo, J. Jaramillo, R. Gomperts, R. E. Stratmann, O. Yazyev, A. J. Austin, R. Cammi, C. Pomelli, J. W. Ochterski, R. L. Martin, K. Morokuma, V. G. Zakrzewski, G. A. Voth, P. Salvador, J. J. Dannenberg, S. Dapprich, A. D. Daniels, O. Farkas, J. B. Foresman, J. V. Ortiz, J. Cioslowski, and D. J. Fox, *Gaussian* 09, *Revision* A.02 (Gaussian Inc., Wallingford CT, 2009).
[26]T. H. Dunning, Jr., J. Chem. Phys. **90**, 1007 (1989).
[27]J. Cizek, Adv. Chem. Phys. **14**, 35 (1969).
[28]G. E. Scuzeria and H. F. Schaefer III, J. Chem. Phys. **90**, 3700 (1989).
[29]Y. Zhao and D. G. Truhlar, Theor. Chem. Acc. **120**, 215 (2008).
[30]C. Van Caillie and R. D. Amos, Chem. Phys. Letters. **317**, 159 (2000).
[31]T. Shimanoushi, *Tables of Molecular Vibrational Frequencies. Consolidated* Volume I, NSRDS-NBS 39, 1972, U.S.Gov.Print.Off., Washington DC 20402.
[32]R. F. Lake and H. Thompson, Proc. Roy. Soc. London A **315**, 323 (1970).
[33]K. Wittel and H. Bock, Chem. Ber. **107**, 317 (1974).
[34]W. Von Niessen, L. Åsbrink, and G. Bieri, J. Electr. Spectry. Rel. Phenom. **26**, 173 (1982).
[35]K.-C. Lau, H. K. Woo, P. Wang, X. Xing, and C. Y. Ng, J. Chem. Phys. **124**, 224311 (2006).
[36]M. A. Parkes, S. Ali, C. R. Howle, R. P. Tuckett, and A. E. R. Malins, Mol. Phys. **105**, 907 (2007).
[37]R. Locht, B. Leyh, K. Hottmann, and H. Baumgärtel, Chem. Phys. **220**, 207 (1997).
[38]G. Tornow, R. Locht, R. Kaufel, H. Baumgärtel, and H.-W. Jochims, Chem. Phys. **146**, 115 (1990).
[39]R. Locht, B. Leyh, A. Hoxha, H.-W. Jochims, and H. Baumgärtel, Chem. Phys. **272**, 259 (2001); R. Locht, B. Leyh, H.-W. Jochims, and H. Baumgärtel, *ibid.* **317**, 73 (2005); **365**, 109 (2009).
[40]R. Locht, B. Leyh, D. Dehareng, H.-W. Jochims, and H. Baumgärtel, Chem. Phys. **362**, 97 (2009).
[41]R. Locht, H. W. Jochims, and B. Leyh, Chem. Phys. **405**, 124 (2012).
[42]R. Locht, D. Dehareng, and B. Leyh, Mol. Phys. **112**, 1520 (2014).